Article:

Han, Yaofei, Chen, Shaofeng, Ma, Zhixun et al. (3 more authors) (2024) Search-Algorithm-Based Offline Inductance Identification Using Sliding Mode Flux Observation Data for IPMSMS. IEEE/ASME Transactions on Mechatronics. ISSN: 1941-014X

https://doi.org/10.1109/TMECH.2023.3348139

Novel Search-Algorithm-based Offline Inductance Identification Using Sliding Mode Flux Observation Data for IPMSMs

Yaofei Han, Shaofeng Chen, Zhixun Ma, Chao Gong, Xing Zhao, Yunwei Li

***Abstract*—This paper proposes a sliding mode observer (SMO)-based technique to detect the *d, q*-axis inductances of interior permanent magnet synchronous machines (IPMSM) offline by using a novel search algorithm. The rationale behind the proposed method is that the chattering effects of the SMO are minimal when the parameters used to construct the observer comply with the real ones. First, a sliding mode flux observer (SMFO) is constructed to observe the rotor flux that has strong links with the inductances. Second, the relationship between the inductances and the observed flux, which is relevant to the chattering effects of the SMFO, is illustrated in theory. Then, a quick search algorithm that can be easily executed on the digital processors is designed to detect the *d, q*-axis inductances. Finally, comparative experiment is conducted on an IPMSM to validate the proposed techniques.**

***Index Terms*— Interior permanent magnet synchronous motor, sliding mode flux observer, chattering, offline inductance, parameter identification.**

I. INTRODUCTION

INTERIOR permanent magnet synchronous machines (IPMSM) are widely adopted in electric vehicles, aircraft, and railways, etc., due to the advantages of high-power density, high efficiency, and compact structure [1]. IPMSM is a nonlinear system with strong coupling and to clearly describe its electrical and mechanical properties, a set of differential equations needs to be used to constitute the machine model [2]. Apart from the motor states, parameters including inductance, rotor flux, resistance, rotor inertia, and damping are crucial for the machine model. This leads to the fact that it is necessary to obtain the machine parameters before achieving the model-based analysis or control techniques.

From the perspective of application modes, the machine parameters can be categorized into offline parameters and online parameters [3]. Specifically, the offline parameters refer to those detected before they are used, while the online ones are applied instantaneously after they are detected. Comparatively, at the stage of motor analysis or control, the offline parameters occupy no computing resources so as not to conflict with the main task. However, as for the online parameters, because they need to be identified in real time, long calculation time resulting from the parameter identification algorithms is inevitable. In this case, it is hard to achieve satisfying control performance through control period optimization [4].

In engineering, the offline motor parameters can be obtained by using direct offline identification (DOI) or consulting online identification (OI) strategies [5-11]. One common DOI method employs physical instruments to detect the parameters of the motionless motors. For example, the inductance and resistance can be measured using a multimeter [5]. Nevertheless, it is hard for this strategy to distinguish the *d*, *q*-axis inductances of IPMSMs because they are strongly coupled. To solve the issue, high-frequency signals can be injected into the static motor, and the response signals are further used to calculate the *d*, *q*-axis inductances [6]. However, this strategy requires specific band-pass filters, increasing the complexity of the whole system. In terms of the OI methods, they are only applicable while the motor is rotating. The commonly used OI techniques include feature extraction based on signal analysis [7], sliding mode observer (SMO)-based estimation [8-10], extended Kalman filter (EKF)-based estimation [11], recursive least square-(RLS) based estimation [12], model reference adaptive system (MRAS)-based estimation [13], and artificial intelligence (AI)-based estimation [14], etc. Because the OI strategies are able to identify and record the *d*-axis and *q*-axis inductances discretely, they are well-suited for collecting offline inductances.

Among those OI strategies, SMOs are characterized by fast response and simple structure [15], thereby deserving further investigation. However, there exist two problems when using the traditional sliding mode inductance observers (SMIO) to identify the *d*, *q*-axis inductances [8], [16], [17]. First, a priori *q*-axis inductance value, which might be inaccurate, is required to establish the *d*-axis inductance observer and vice versa. Undoubtedly, this will lower the identification accuracy. Second, the intrinsic property (namely, chattering) of the SMOs is usually treated as a factor degrading the system performance and low-pass filters need to be employed to suppress the chattering effects. So far, although many studies concerning SMOs have revealed the characteristics of chattering [18], few of them try to take full advantage of this property.

To solve the aforementioned issues, this paper proposes a new search algorithm that relies on a sliding mode flux observer (SMFO) to identify the offline inductances. The contributions of the proposed method can be summarized as follows. First, although the *d, q*-axis inductances are the final parameters to be identified, an SMFO is developed in this paper rather than SMIOs. The *d*, *q*-axis inductances are obtained by searching for their values minimizing the fluctuations of the flux observation results. For the proposed method, it can achieve high accuracy in estimating the inductances regardless of the a priori parameter values. Second, the chattering of the proposed SMFO does not need to be tackled. Instead, it is innovatively utilized identify the machine parameters. Compared to the traditional SMIOs, the novelties of proposed inductance identification methods reflect in both its rationale and implementations. 1) Rationale: The proposed method is achieved by addressing the chattering effects in the SMFOs caused by mismatched inductances or uncertainties. By identifying inductance values that minimize chattering, the method obtains inductance estimates that closely align with real-world values. This is achieved by devising efficient search algorithms that measure and evaluate the fluctuations induced by inductance-related chattering. 2) Implementations: Quick search algorithms based on the golden ratio principle, which can be directly executed in the digital processors (DP), are designed to obtain the accurate d, q-axis inductance values. The proposed method contributes to enriching the theories concerning parameter identification of IPMSMs. Experimental results prove that the proposed strategy is effective.

II. Structure of SMFO

The electrical property of IPMSM in q-axis reference frame, which contains the flux information, is described as follows:

$$\frac{\mathrm{d}i_q}{\mathrm{d}t} = -\frac{L_d}{L_q} p\omega_m i_d - \frac{R_s}{L_q} i_q + \frac{u_q}{L_q} - \frac{\psi_f}{L_q} p\omega_m \quad (1)$$

where i_d, i_q are d, q-axis currents; R_s is resistance; p is the number of pole pairs; u_q is q-axis control voltage; L_d, L_q are the d, q-axis inductances; ω_m is angular speed; ψ_f is rotor flux. Here, it is reasonable to assume that the resistance R_s can be obtained accurately by using offline or online methods considering that flux and inductances are the targeting objectives to be studied.

Based on the SM variable structure theory and (1), the SMFO can be designed as follows:

$$\frac{\mathrm{d}i_q^*}{\mathrm{d}t} = -\frac{L_d}{L_q} p\omega_m i_d - \frac{R_s}{L_q} i_q^* + \frac{u_q}{L_q} - \frac{\lambda F(\bar{i}_q)}{L_q} p\omega_m \quad (2)$$

where i_q^* is the estimated current of the SMFO; $\bar{i}_q$ is the error between the estimated current and the measured current, namely, $\bar{i}_q = i_q^* - i_q$, and $F(\bar{i}_q)$ is the switching function:

$$F(\bar{i}_q) = \frac{1-e^{-\bar{i}_q}}{1+e^{-\bar{i}_q}} \quad (3)$$

λ is gain factor, and it should satisfy the following condition to make the SMFO stable:

$$\begin{cases} \lambda F(\bar{i}_q) - \psi_f > 0, if\ \bar{i}_q > 0 \\ \lambda F(\bar{i}_q) - \psi_f < 0, if\ \bar{i}_q < 0 \end{cases} \rightarrow \lambda > \left|\frac{\psi_f}{F(\bar{i}_q)}\right| \quad (4)$$

Referring to [19], there must be a positive constant satisfying (5) when the concept of estimation error is taken into account. When the SMFO arrives at an equilibrium state, the observed flux ψ_f^* can be deduced as:

$$\psi_f^* = \lambda F(\bar{i}_q) \quad (5)$$

III. Flux Observation-Data-based Inductance Identification Using Quick-Search-Algorithm

This part introduces the relationship between inductance mismatch and flux observation results first, laying the foundation for developing a search algorithm-based parameter identification method. Then, in order to utilize the flux estimation results for inductance identification, a quick search algorithm based on the golden ratio principle is presented for inductance identification.

A. Relationship Between Inductance Mismatch and Flux Observation Results

When adopting the proposed SMFO to observe the flux linkage, a priori d, q-axis inductances need to be substituted into (2) for calculation. However, if the inductances are mismatched, the observed flux results are significantly different due to the chattering caused by the inertial delay effect [18]. Specifically, the flux estimation fluctuations (FEF) that are defined as (6) increase as the mismatch degree rises.

$$\psi_{f\_\text{flu}} = \psi_{f\_\max} - \psi_{f\_\min} \quad (6)$$

where ψ_{f_flu} is the value of FEF, $\psi_{f\_\max}$ and $\psi_{f\_\min}$ are the maximum and minimum estimated flux values within a certain period, respectively. Based on the above explanations, when the inductances used in the SMFO match the true real-world values, the FEFs are minimized due to the reduced chattering effects. Hence, the inductances minimizing the FEFs equal the true real-world values, which can be obtained through search algorithms. This is the theoretical foundation for the proposed inductance detection technique.

B. Proposed Quick Search Algorithm-Based Inductance Identification

The proposed search algorithm contains two sequential parts: q-axis inductance detection and d-axis inductance detection, which are detailed as follows:

a) q-axis inductance detection

Assuming that the inductance identification algorithms are launched from the kth control period, the execution procedures with the initial and ending conditions integrated are illustrated in Fig. 1.

First, within the kth period, three steps are included:

S_1: *Initial condition setting*: As for a PMSM, although the accurate inductances are unknown, they can be empirically assumed by engineers. On this basis, the appropriate initial conditions including a priori d-axis inductance L_{d0} and the search area of the q-axis inductance ($L_{q\_\min}$ and $L_{q\_\max}$) need to be given. In this paper, L_{d0} = 0.01, $L_{q\_\min}$ =0.001 and $L_{q\_\max}$ =0.07. Besides, two indexing variables i (counting with the control period) and j are set to 0, and the number of control periods used for fluctuation calculation (N) is determined.

S_2: *Feature point selection*: Apart from $L_{q\_\min}$ and $L_{q\_\max}$, based on the golden ratio and median methods, three more points (L_{q_g1}, L_{q_m} and L_{q_g2}) that need to be evaluated are selected, that is,

$$\begin{cases} L_{q\_g1} = 0.618L_{q\_\min} + 0.382L_{q\_\max} \\ L_{q\_m} = 0.5L_{q\_\min} + 0.5L_{q\_\max} \\ L_{q\_g1} = 0.382L_{q\_\min} + 0.618L_{q\_\max} \end{cases} \quad (7)$$

S_3: *Flux estimation using the SMFO*: Employ L_{d0} together

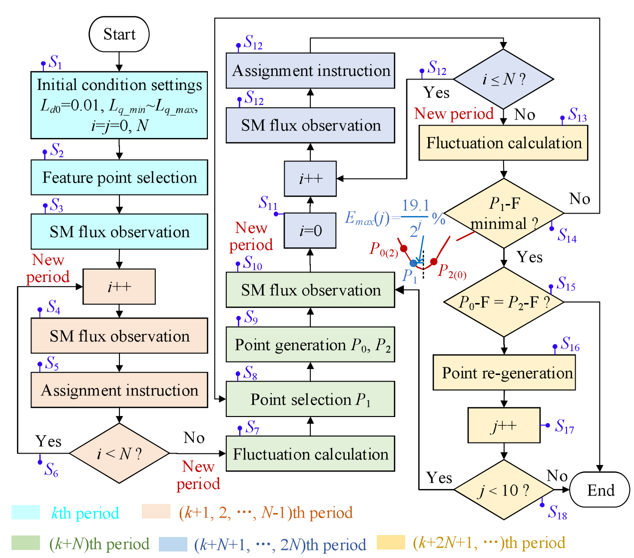

Fig. 1. q-axis inductance search algorithms.

with $L_{q\_\min}$, L_{q_g1}, L_{q_m}, L_{q_g2} and $L_{q\_\max}$ to estimate five sets of flux values using the SMFO (2).

Second, after the kth period is completed, the following steps are executed between the $(k+1)$th and the $(k+N-1)$th periods:

S_4: *Flux estimation*: This stage is the same as S_3 but the estimated flux is different from S_3.

S_5: *Assignment instruction*: In the $(k+i)$th period, compare the five groups of estimated flux with the corresponding ones in the previous period. Then, select the maximum and minimum flux and assign them to $\psi_{f\_\max}$ and $\psi_{f\_\min}$, respectively.

S_6: *Repeat S_4 and S_5*: Repeat S_4 and S_5 until the $(k+N-1)$th period is completed.

Third, within the $(k+N)$th period, four steps are included:

S_7: *Fluctuation calculation*: Since $\psi_{f\_\max}$ and $\psi_{f\_\min}$ have been obtained in the previous periods, the FEFs corresponding to the five sets of inductance values can be calculated by using (6).

S_8: *Point selection*: Select the q-axis inductance which minimizes fluctuations from the five inductance values in S_2. Treat it as the one closest to the real inductance and denote it as P_1.

S_9: *Point generation*: Based on the golden ratio method, in addition to P_1, two more points (P_0 and P_2) near it are generated, which can be represented as:

$$P_0 = 0.618P_1, P_2 = 1.382P_1 \tag{8}$$

S_{10}: *Flux estimation*: Use L_{d0} together with P_0, P_1 and P_2 to estimate three groups of flux using the SMFO.

Fourth, between the $(k+N+1)$th and the $(k+2N)$th period, the following steps are implemented:

S_{11}: *Resetting i*: Reset the value of i to 0 immediately when the $(k+N+1)$th period starts.

S_{12}: *ψ_{f_max} and ψ_{f_min} calculation*: Execute the operations in S_{10}, S_5 and S_6 until the $(k+2N)$th period is completed to obtain the new $\psi_{f\_\max}$ and $\psi_{f\_\min}$ values.

Fifth, after the $(k+2N)$th period, the execution procedures are as follows:

S_{13}: *Fluctuation calculation*: Use the $\psi_{f\_\max}$ and $\psi_{f\_\min}$ values in S_{12} to calculate the FEFs corresponding to the three sets of inductance values.

S_{14}: *Evaluation of P_1*: Since P_1 is situated between P_0 and P_2, the ending conditions can be simplified by ensuring that the FEF corresponding to P_1 ($P_{1\text{-}F}$) is minimized. Hence, in this step, judge whether this goal is achieved. If it is not achieved, repeat the operations in S_8~S_{14} relying on P_0, P_1 and P_2; Otherwise, execute S_{15}. It deserves to be mentioned when the P_1-F stands at the lowest position for the first time ($j = 0$), the maximum deviation ratio of P_1 from the real inductance ($E_{\max}$) is:

$$E_{\max}(j)\big|_{j=0} = \frac{\dfrac{P_1(1+1.382)}{2} - P_1}{P_1} \times 100\% = 19.1\% \tag{9}$$

S_{15}: *Evaluation of P_0 and P_2*: Assume that the FEFs are equal when the distance from the real inductance value is the same. Then, if the FEFs corresponding to P_0 and P_2 (P_0-F and P_2-F) are equal, the average (*ave*) of them is the real inductance. Hence, 'P_0-F=P_2-F' can be treated as one ending condition. In this case, the estimated q-axis inductance L_q^* is:

$$L_q^* = \frac{P_0 + P_2}{2} \tag{10}$$

S_{16}: *Point re-generation*: If P_0-F does not equal P_2-F, generate new points P_0 and P_2 based on the following condition:

$$P_0 = P_1(1 - E_{\max}(j)), P_2 = P_1(1 + E_{\max}(j)) \tag{11}$$

S_{17}: *Change of j*: 1 is added to j and a new j is obtained.

S_{18}: *Calculation of P_1 tenfold*: Repeat the operations in S_{10}~S_{17} until j equals 10 (another ending condition). Now, $E_{\max}$ shown in (12) is small enough theoretically, and then, P_1 can be treated as the estimated inductance:

$$E_{\max}(j)\big|_{j=10} = 0.018\%, L_q^* = P_1 \tag{12}$$

b) *d*-axis inductance detection

When the q-axis inductance is identified, L_q^* is regarded as a priori condition of the d-axis inductance identification algorithm, which is the main difference from the current algorithms. Except for this, the operations comply with S_1~S_{18} when estimating the d-axis inductance L_d^*.

TABLE I
PARAMETERS OF IPMSM PROTOTYPE

Parameter	Value	Unit
stator winding resistance R_s	0.605	Ω
measured d-axis inductance L_{d_m}	12.65	mH
measured q-axis inductance L_{q_m}	13.5	mH
the number of pole pairs p	2	-
flux linkage ψ_f	0.6873	Wb

IV. Verification Results

To validate the proposed search algorithm-based offline inductance identification strategy, experiment is conducted on an IPMSM prototype. The d, q-axis inductances of the test motor can be accurately measured by the signal-injection-based OI method, which are given in Table I. In this paper, the measured inductances (L_{d_m} and L_{q_m}) in Table I are regarded as the accurate ones. The dc-bus voltage is 150 V. The proposed algorithms are implemented on a dSPACE control board, and data are recorded by the dSPACE Control Desk. A load motor that works under the torque control mode is coupled to the test IPMSM to provide the required load. For the purpose of comprehensiveness, experiment is divided into two parts. First, the FEFs under different inductances are presented to illustrate the impacts of the chattering, proving that the theoretical foundation of this study is correct. Second, the d, q-axis inductance estimation results are given to prove that the

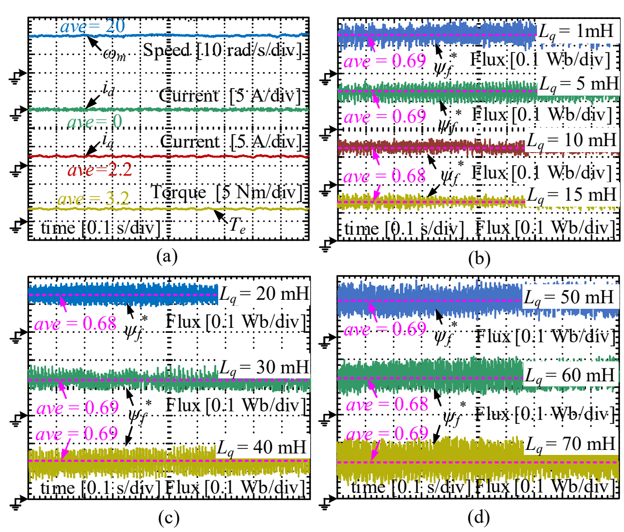

Fig. 2. Experimental results when d-axis inductance is set as 10 mH while q-axis inductance changes from 1 mH to 70 mH. (a) States of motor. (b) Flux estimation results. (c) Flux estimation results. (d) Flux estimation results.

TABLE II
VALUES OF FEFS CORRESPONDING TO VARIOUS INDUCTANCES

L_d(mH)	L_q (mH)	$\psi_{f\ \min}$ (Wb)	$\psi_{f\ \max}$ (Wb)	$\psi_{f\ \mathrm{flu}}$ (Wb)
10	1	0.4	0.95	0.55
10	5	0.43	0.89	0.46
10	10	0.53	0.87	0.34
10	15	0.54	0.85	0.31
10	20	0.43	0.88	0.45
10	30	0.39	0.89	0.50
10	40	0.33	0.93	0.60
10	50	0.33	1.04	0.71
10	70	0.24	1.08	0.84

proposed search algorithm is effective. In the process, apart from the inductances obtained by the OI method, the results of the traditional SMIOs in [8] are presented for comparison.

A. Impacts of Chattering on FEFs

To reveal the impacts of chattering on the FEFs, assume that either the *d*-axis inductance or the *q*-axis inductance used to construct the SMFO is fixed and the flux estimation results are recorded when the other inductance changes.

Fig. 2 shows the results when the *d*-axis inductance equals the initial condition of the search algorithm (L_{d0} = 10 mH), while the *q*-axis inductance changes from 1 mH to 70 mH. By varying the *d*-axis inductance instead of using the exact value in Table I, a stronger and more conclusive validation of the proposed algorithm's performance can be established. Fig. 2(a) indicates that the motor rotates at 20 rad/s under the load of 3 Nm. Fig. 2(b) - Fig. 2(d) address two phenomena that require attention. First, the FEFs corresponding to various *q*-axis inductances are different. As shown in Table II, as the inductance deviations become more pronounced, the FEFs exhibit a corresponding increase. These comply with the theoretical analysis in Section II-*B*. Second, the estimated flux values are either 0.68 Wb or 0.69 Wb. It is worth mentioning that the SMFO shows relatively strong robustness against *q*-axis inductance variations. This behavior can be attributed to the fact that the *d*-axis current remains constant at zero during the experiment [8].

B. Inductance Identification Results

a) Proposed method

When the motor works under conditions depicted in Fig. 2(a), the flux estimation results of the proposed search algorithms, which correspond to the final three points (j = 10) evaluated for *q*, *d*-axis inductances, are depicted in Fig. 3(a) and Fig. 3(b), respectively. Based on (11), the estimated *q*-axis inductance L_q^* is 14.4 mH and the *d*-axis inductance L_d^* is 12.3 mH. These

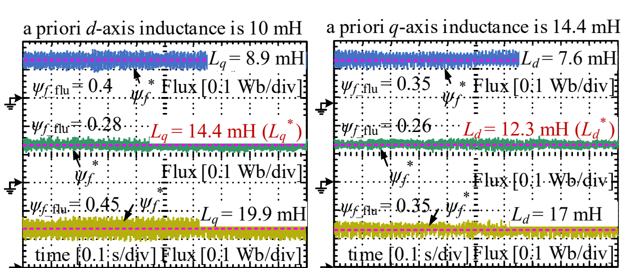

(a) (b)

Fig. 3. Experimental results of proposed method at 20 rad/s and 3 Nm. (a) Flux estimation results corresponding to final three points when search algorithm is executed for *q*-axis inductance estimation. (b) Flux estimation results corresponding to final three points when search algorithm is executed for *d*-axis inductance estimation.

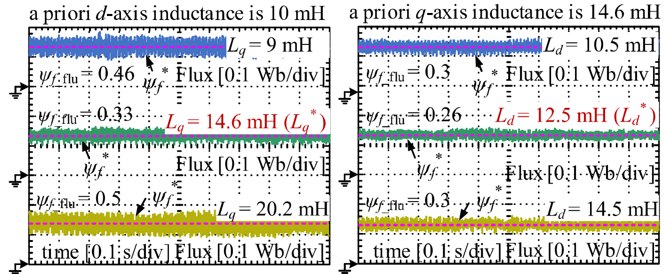

(a) (b)

Fig. 4. Experimental results of proposed method at 30 rad/s and 3 Nm. (a) Flux estimation results corresponding to final three points when search algorithm is executed for *q*-axis inductance estimation. (b) Flux estimation results corresponding to final three points when search algorithm is executed for *d*-axis inductance estimation.

values ensure that the SMFO generates lower fluctuations. However, their deviation ratios stand at 6.7% and 2.7%, respectively, which are slightly higher compared to the value stated in equation (12). The reason behind this discrepancy may lie in the inaccuracy of the measurement values. Despite this, in general, this method can still demonstrate good estimation accuracy even though the a priori inductances do not equal the real-world values.

When the motor rotates at 30 rad/s under 3 Nm and i_d = 0, the flux estimation results obtained from the proposed search algorithms are displayed in Fig. 4 for the final three points. The estimated *q*-axis inductance L_q^* is 14.6 mH, which is similar to that in Fig. 3. In terms of the *d*-axis inductance, based on (10), the estimated value is 12.5 mH, which is close to the accurate inductance presented in Table I.

b) Traditional SMIOs

To clearly demonstrate the advantages of the proposed method, the traditional SMIOs are employed for comparison. To make the SMIOs stable, the *d*-axis current should not be zero [8]. Hence, although the motor still operates at the speed of 20 rad/s and under the load of 3 Nm, the *d*-axis current is controlled to maintain at 1.0 A during the test. Notably, this approach differs from the configurations in Fig. 2(a).

On the one hand, when the a priori *d*, *q*-axis inductances used for the SMIOs comply with the accurate values presented in Table I, Fig. 5 shows the estimation results. The estimated *d*-axis inductance $L_{d\_\mathrm{SMIO}}^*$ is 12.3 mH, which is only 3.7% different from the real value. Similarly, the estimated *q*-axis inductance $L_{q\_\mathrm{SMIO}}^*$ is 14 mH, which is 2.7% different from the actual value. In this scenario, the estimation results of the traditional SMIOs demonstrate high accuracy.

On the other hand, when the a priori *d*, *q*-axis inductance values used for the SMIOs are inaccurate, being two times larger than those in Table I, the inductance estimation results

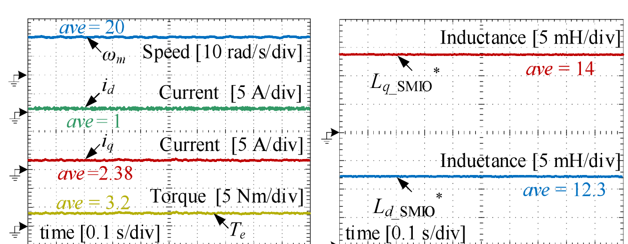

(a) (b)

Fig. 5. Experimental results of traditional SMIOs with accurate a priori parameters. (a) States of motor when SMIOs are implemented. (b) Inductance estimation results of traditional SMIOs.

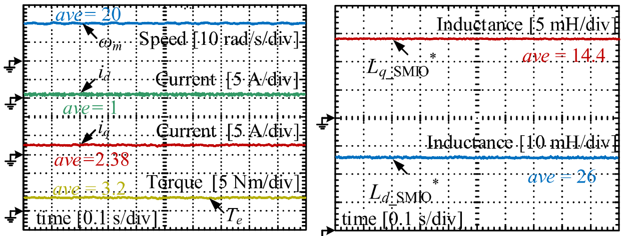

(a) (b)

Fig. 6. Experimental results of traditional SMIOs with inaccurate a priori parameters. (a) States of motor when SMIOs are implemented. (b) Inductance estimation results of traditional SMIOs.

are depicted in Fig. 6. It can be seen that the estimated *d*, *q*-axis inductances are 26 mH and 14.4 mH, which are 105% and 6.7% different from the real values. It is evident that compared to the results in Fig. 5, the estimation accuracy reduces significantly when using inaccurate a priori inductance values, especially for the *d*-axis inductance.

Overall, the proposed inductance estimation method exhibits robust performance across various working conditions and a priori parameter settings. It consistently demonstrates good accuracy in estimating the inductance values. However, the traditional SMIOs perform well only when the a priori parameters are close to the real values, as also confirmed in [8]. Comparatively, the advantage of the proposed method lies in its ability to be less reliant on the accuracy of a priori conditions. This makes it more versatile and reliable, as it can still provide accurate estimations even when the initial parameter values are not precisely known.

V. Conclusion

Based on the relationship between the FEFs caused by the chattering effects of the SMFO and the mismatched inductances, this paper proposes a quick search algorithm to detect the *d*, *q*-axis inductances for IPMSMs. By contrast with the traditional inductance identification methods such as SMIOs, the new method takes full advantage of the chattering effects of the SMOs. Therefore, the main novelty of this study lies in the creation of an entirely new technology dedicated to addressing the parameter identification challenge. By virtue of the proposed search algorithm that can be easily executed in the DPs, the *d*, *q*-axis inductance values can be detected accurately. The advantage of the proposed method reflects in that no accurate a priori parameters are needed. The contribution extends to the field of parameter identification, providing a practical and effective solution to accurately determine inductance values, thereby enhancing the analysis and control of IPMSMs in various applications. Experimental results prove that the theoretical foundation of this study and the proposed search algorithm are effective.

References

[1] B. Shuang, Z. Q. Zhu and X. Wu, "Improved Cross-coupling Effect Compensation Method for Sensorless Control of IPMSM With High Frequency Voltage Injection," *IEEE Trans. Energy Convers.*, vol. 37, no. 1, pp. 347-358, March 2022.

[2] Z. -H. Liu, J. Nie, H. -L. Wei, L. Chen, F. -M. Wu and M. -Y. Lv, "Second-Order ESO-Based Current Sensor Fault-Tolerant Strategy for Sensorless Control of PMSM With B-Phase Current," in *IEEE/ASME Trans. Mechatron.*, vol. 27, no. 6, pp. 5427-5438, Dec. 2022.

[3] X. Wu, X. Fu, M. Lin and L. Jia, "Offline Inductance Identification of IPMSM With Sequence-Pulse Injection," *IEEE Trans. Ind. Inform.*, vol. 15, no. 11, pp. 6127-6135, Nov. 2019.

[4] H. A. Young, M. A. Perez and J. Rodriguez, "Analysis of Finite-Control-Set Model Predictive Current Control With Model Parameter Mismatch in a Three-Phase Inverter," *IEEE Trans. Ind. Electron.*, vol. 63, no. 5, pp. 3100-3107, May 2016.

[5] D. Uzel and Z. Peroutka, "Optimal Control and Identification of Model Parameters of Traction Interior Permanent Magnet Synchronous Motor Drive," *IECON 2011 - 37th Annual Conference of the IEEE Industrial Electronics Society*, 2011, pp. 1960-1965.

[6] Q. Wang, G. Wang, S. Liu, G. Zhang and D. Xu, "An Inverter-Nonlinearity-Immune Offline Inductance Identification Method for PMSM Drives Based on Equivalent Impedance Model," in *IEEE Trans. Power Electron.*, vol. 37, no. 6, pp. 7100-7112, June 2022.

[7] K. Wang *et al*, "Rotor Temperature Estimation for Magnetically Suspended Turbo Molecular Pump Based on Flux Linkage Identification," in *IEEE/ASME Trans. Mechatron.*, vol. 27, no. 6, pp. 5780-5791, Dec. 2022.

[8] Y. Han, G. Chen, Z. Ma and S. Chen, "Robust MTPA Control for Novel EV-WFSMs based on Pure SM Observer-based Multistep Inductance Identification Strategy," *IEEE Trans. Ind. Electron.*, vol. 69, no. 12, pp. 12390-12401, Dec. 2022.

[9] W. Zhao, X. Ren and S. Wang, "Parameter Estimation-Based Time-Varying Sliding Mode Control for Multimotor Driving Servo Systems," in *IEEE/ASME Trans. Mechatron.*, vol. 22, no. 5, pp. 2330-2341, Oct. 2017.

[10] M. H. Choi, B. Shirinzadeh and R. Porter, "System Identification-Based Sliding Mode Control for Small-Scaled Autonomous Aerial Vehicles With Unknown Aerodynamics Derivatives," in *IEEE/ASME Trans. Mechatron.*, vol. 21, no. 6, pp. 2944-2952, Dec. 2016.

[11] X. Li and R. Kennel, "General Formulation of Kalman-Filter-Based Online Parameter Identification Methods for VSI-Fed PMSM," *IEEE Trans. Ind. Electron.*, vol. 68, no. 4, pp. 2856-2864, April 2021.

[12] A. Brosch, S. Hanke, O. Wallscheid and J. Böcker, "Data-Driven Recursive Least Squares Estimation for Model Predictive Current Control of Permanent Magnet Synchronous Motors," *IEEE Trans. Power Electron.*, vol. 36, no. 2, pp. 2179-2190, Feb. 2021.

[13] X. An, G. Liu, Q. Chen, W. Zhao and X. Song, "Adjustable Model Predictive Control for IPMSM Drives Based on Online Stator Inductance Identification," *IEEE Trans. Ind. Electron.*, vol. 69, no. 4, pp. 3368-3381, April 2022

[14] Z. Wang, J. Chai, X. Xiang, X. Sun and H. Lu, "A Novel Online Parameter Identification Algorithm Designed for Deadbeat Current Control of the Permanent-Magnet Synchronous Motor," *IEEE Trans. Ind. Appl.*, vol. 58, no. 2, pp. 2029-2041, March-April 2022.

[15] S. S. Patil, V. Wanaskar, P. D. Shendge and S. B. Phadke, "Sliding Mode and Inertial Delay Based Direct Yaw Moment Control for AGVs," *2021 6th International Conference for Convergence in Technology (I2CT)*, Maharashtra, India, 2021, pp. 1-6.

[16] W. Wang, J. Ma, Z. Cheng, X. Li, C. W. d. Silva and T. H. Lee, "Global Iterative Sliding Mode Control of an Industrial Biaxial Gantry System for Contouring Motion Tasks," in *IEEE/ASME Trans. Mechatron.*, vol. 27, no. 3, pp. 1617-1628, June 2022.

[17] S. Jeong and D. Chwa, "Sliding-Mode-Disturbance-Observer-Based Robust Tracking Control for Omnidirectional Mobile Robots With Kinematic and Dynamic Uncertainties," in *IEEE/ASME Trans. Mechatron.*, vol. 26, no. 2, pp. 741-752, April 2021.

[18] M. R. Soltanpour and S. Zaare *et al.* "Free-Chattering Fuzzy Sliding Mode Control of Robot Manipulators with Joints Flexibility in Presence of Matched and Mismatched Uncertainties in Model Dynamic and Actuators," *J. Intell. Robot. Syst.,* vol. 100, no. 1, pp. 47–69, April 2020.

[19] C. Gong and Y. Hu *et al*, "An Improved Delay-Suppressed Sliding-Mode Observer for Sensorless Vector-Controlled PMSM," *IEEE Trans. Ind. Electron.*, vol. 67, no. 7, pp. 5913-5923, July 2020.